Nondestructive Determination of the Lateral Thermal Conductivity of Novel Substrate Materials using Thermal Infrared Microscopy

E. R. Heller[a], K. Chabak[b], V. Miller[b], D. Walker Jr.[b], M. Trejo[b], M. Kossler[b], J.K. Gillespie[b], A. Crespo[b], R. Vetury[c], G.D. Via[b]

[a]Air Force Research Laboratory, Materials Directorate, Wright-Patterson Air Force Base, OH 45433, USA
[b]Air Force Research Laboratory, Sensors Directorate, Wright-Patterson Air Force Base, OH 45433, USA
[c]RFMD, Defense and Power, Charlotte, NC, 28269, USA

HEMT, GaN, IR microscopy, Thermal Conductivity, Temperature Measurement, Diamond

Abstract

The lateral thermal conductivity of substrates was probed with IR thermal microscopy. We show that heat spreading can be measured with useable accuracy, on-wafer and non-destructively through measurements on Si, SiC and a novel diamond substrate. Sources of error are investigated and discussed.

INTRODUCTION

IR thermal microscopy is a tool that is available to many groups and is inherently passive, quick, and non-destructive. However, the shortcomings of this technique for sub-micron scale temperature measurement within an active Wide Bandgap (WBG) device are well known [1, 2]. Some of these known issues are alleviated by restricting IR thermal measurements to regions that are opaque in the IR, with significant emissivity and with a low enough thermal gradient that the existing spatial resolution of the instrument is sufficient. We show that this measurement configuration is suitable for the in-plane thermal conductivity of the substrate (or of the substrate/epi combination if those layers are thick enough to affect heat spreading).

Specifically, we measured the thermal conductivity of Si, SiC and diamond, some as a function of temperature. All measurements utilized the existing test structures; no custom patterns or test wafers were needed. Comparison with known data (Si and SiC) provides an objective measure of the accuracy of the technique. Repeated measurements and variation of the test structure, the measurement conditions and the probing method provide insight into the precision (repeatability) and sources of error. Modeling is used to understand additional errors and validate the overall method. Finally, the technique is used on a diamond wafer, for which the temperature dependent thermal conductivity is reported.

EXPERIMENT

An aluminum chuck was constructed with a 3.0 mm diameter hole and a surrounding vacuum ring of about 20 mm diameter. Figure 1 shows a cross section through a 3D model (ANSYS) [3] of this arrangement. A wafer is placed on the chuck with a source of heat in the very center of the central hole (a device or test structure with bias applied). Heat is forced flow from the device, through the wafer, and into the chuck. Briefly, by measuring the temperature differences sustained across the wafer the thermal conductivity of the host wafer can be measured. To test for sensitivity in wafer-chuck thermal resistance, the ring was sometimes connected to vacuum and sometimes not, but the central hole was always vented to the ambient. Effects of non-uniform wafer-chuck thermal resistance and of changes to the vacuum applied are discussed in the results section.

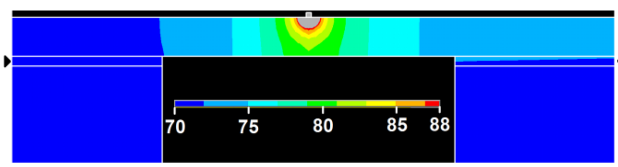

Figure 1: A modeled cross section of a rectangular heat source of 50 by 150 µm size on a SiC wafer on the chuck described at 70 °C. In this example, the left side is shown modeled with the chuck-wafer interface as 500 $kW/m^2/K$ and the right as 1 $kW/m^2/K$ (modeled as the thin layer shown between arrows). This shows the effect of variation in this on the temperature profile. 20 $kW/m^2/K$ is expected with the vacuum on [4].

With this setup, GaN based devices (TLM structures and 1 and 2 finger HEMTs) on Si, SiC and diamond substrates were tested, with wafer thickness varying from 130 µm to 508 µm. All were SiN passivated, on-wafer and using a piece of material at least big enough to cover the 20 mm vacuum ring. In all cases, the heat source was centered in the hole to about 20 µm accuracy with 1-3W DC applied for most tests using tungsten needle probes, Copper Beryllium (CuBe) needle probes or GSG coplanar probes.

Figure 2 shows the temperature distribution expected for a reasonable value of the wafer-chuck thermal resistance. It can be seen in Fig. 1 that after a distance of about the thickness of the wafer from the heat source to near the edge of the hole, the heat is spreading almost purely laterally, such that $dT/dr = P/(2\pi t r \kappa)$, where P is the total dissipated power in the device or test structure, t is the wafer thickness, and κ the temperature dependent thermal conductivity of the wafer. Because the fitted region only covers a few degrees of temperature variation, κ could be approximated as constant within this region as shown by the fitted line.

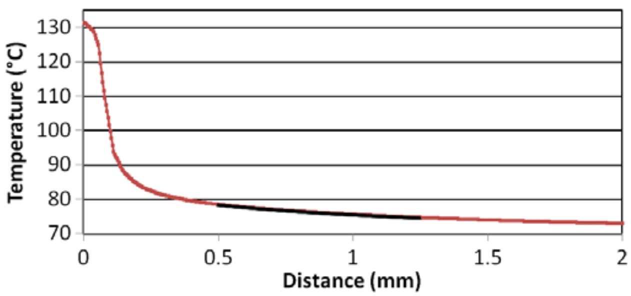

Figure 2: Red line: Modeled temperature from the center of the heat source along the top of the wafer, based on the geometry of Fig. 1 and with 20 $kW/m^2/K$ wafer-chuck resistance. Black line: A fit of $dT/dr = A/r$ to the portion of the profile for which 500 µm < r < 1250 µm, where r = distance from the center of the heat source, where A is a constant. This fit deviates from the model data by less than 0.1 °C within this region.

Figure 3a shows an IR emissivity map of a typical pattern, collected by a QFI Infrascope III [5], where 0 is a perfectly reflecting surface and 1 is a blackbody. It can be seen that there are very low emissivity regions, transparent regions such as unmetalized semiconductor, and regions with metal but with moderate emissivity. Only these last regions are used for the data collection. Specifically, for the rectangular features the median temperature of a small box centered in the rectangle was utilized (corresponding well to the temperature in the center), and the distance used was from the center of the feature to the center of the heat source. For the circular region the process was similar except the data was collected within a small box positioned at that portion of the ring closest to the heat source and separately within a small box positioned at that portion of the ring farthest from the heat source. In other words, two temperature-distance data points came from the ring. With the device powered, Figure 3b shows the temperature map for the same image. Because an IR thermal microscope measures IR intensity radiated from a surface, which is a function of the temperature and emissivity among other things, the temperature measurement is not optimal and is affected by the underlying surface emissivity. It can be seen in Fig. 3b that the best reading comes from opaque regions with the same emissivity, and so *we restrict our data collection only to these portions of the pattern*, and also portions where there is no view of the probes. This is especially important for this experiment because we are measuring dT/dr, and the temperature change was modest for all substrates.

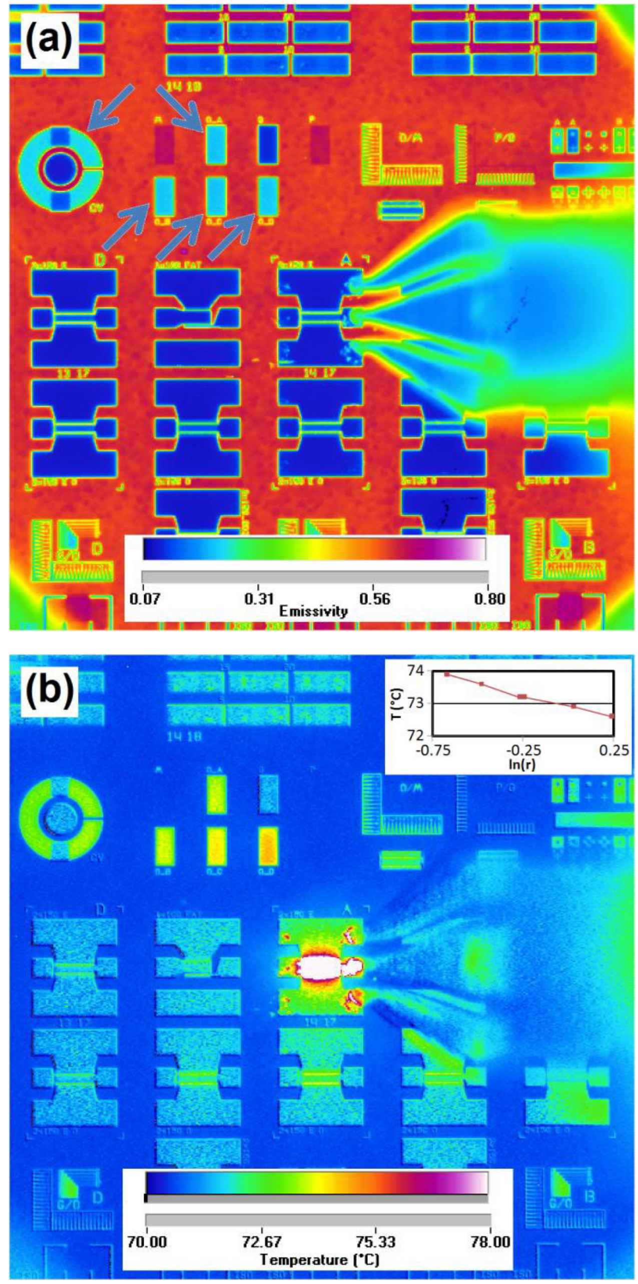

Figure 3: An IR emissivity map (a) and corresponding temperature map (b). Both measure 2400 µm to a side. The arrows show the features on which acceptable data were collected. The emissivity map clearly shows the probes used to power the device; no data can be collected there. The inset shows the plotted temperature vs. natural log of the distance (measured in mm) from the center of the heat source, plotted in this way to make the relationship linear.

Results and Discussion

Figures 4a and 4b show the measurements that were extracted. It is seen that the Si measurements are systematically high, while the SiC data are somewhat low. The Chemical Vapor Deposition (CVD) deposited diamond substrate was polycrystalline, and while the thermal conductivity was expected to be quite good the expected value was unknown.

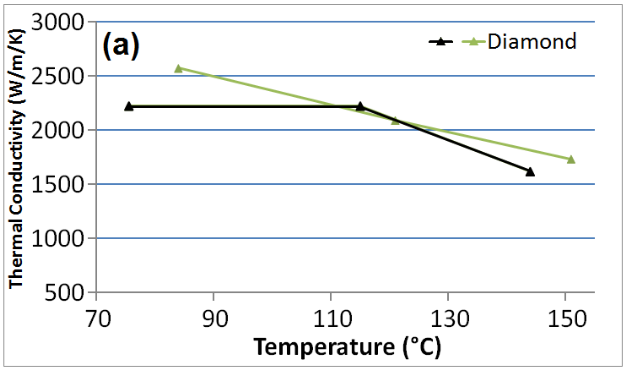

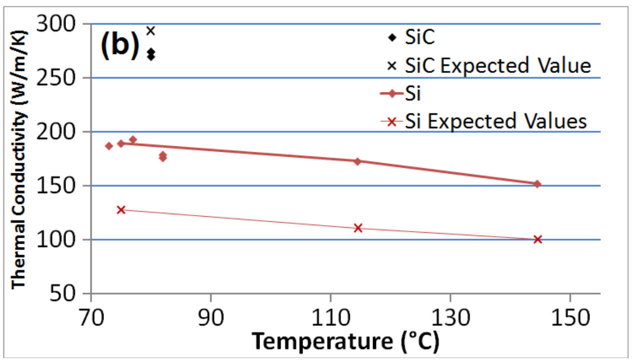

Figure 4: Temperature dependent thermal conductivity data for the wafers tested (diamond, Si and SiC) and compared to expectations for Si and SiC. The diamond data (a) is from two test structures on the same wafer. Multiple data sets exist for each material because of testing under different conditions, although experimental data connected by lines represent data collected under the same conditions except for baseplate temperature.

Numerous factors were investigated as potential contributors to measurement error. First, the actual amount of power dissipating into the wafer must be known. This can be affected by heat leaving through the probes, by ohmic loss in the probes or be other heat conduction paths not involving the wafer, such as air conduction or thermal radiation or lateral conduction through the epilayers or metal layers. Second, the heat conduction path through the wafer must be understood and properly modeled. Third, the temperature measurements themselves must be accurate.

To investigate probe losses, we used GSG coplanar probes by Cascade Microtech, sharpened 175 µm tungsten and sharpened 125 µm CuBe needle probes by GGB Industries. The GSG probes were much blunter than the needle probes and were expected to have less ohmic loss, but should present more of a thermal path for heat loss. While there was some difference in measuring the same sample with different probes it was not clear if this was outside of run-to-run error. Raising and re-landing probes did not affect the measurement much, and probe-probe resistance for the CuBe probes was measured at 1.8 ohm, suggesting that typically 1-2% of the power was dissipated as ohmic loss in the probes (depending on bias conditions), while the GSG probes were less resistive. In addition, data were collected and compared with the HEMT run fully open channel (with the gate floating) and partially pinched off, and on a TLM structure.

Diffusive transport of heat through the air was modeled as a bulk conductor of 0.025W/m/K [6] and not found to affect the result significantly for the wafers studied (this assumption would have to be revised for far thinner or much less conducting materials). Convective transport was ruled out because the volumetric heat capacity of air of about 1.3 $\mu J/mm^3/K$ is insufficient to remove much heat at a reasonable convective flow rate within the region of interest. Lateral thermal transport through epilayers can be dismissed through thickness arguments, although it should be noted that because it is the thickness-conductivity product that is measured this may not have been true for a substrate of poor thermal conductivity. Lateral transport through metals is dismissed by thickness arguments and because the technique developed here relies on the temperature difference between isolated patches of metal. Thermal radiation is easily estimated (up to several mW over the area of the region of interest) and is also not enough to account for the deviation.

There are two aspects to the question of the heat conduction path through the wafer that were investigated. The first is the distance limits over which the lateral transport assumption holds which was discussed already. The second is that the equation $dT/dr = P/(2\pi t r \kappa)$ requires cylindrical symmetry to hold. After about a wafer thickness away from the center of the largest heat source used (2 x 150 µm HEMT) the size of this heat source was not an issue. Large variation in wafer-chuck thermal resistance was modeled and found to be a possible source of error. However, we ran otherwise identical measurements with the vacuum chuck on and off. The wafer would heat up additionally with the vacuum off but the extracted thermal conductivity was found to be about the same because it relies on the temperature difference. We also changed the placement of the wafer on the chuck and changed the placement of the regions of data collection without large effects on the extracted data. We should note that models such as shown in Fig. 1 were constructed for various assumptions for the wafer-chuck thermal resistance, including large variations that violate cylindrical symmetry, and accurate data could still be extracted of the average dT/dr by making temperature measurements with uniform density all the way around the heat source. The already patterned wafers available to us did not allow this, so this was not an option.

The last concern is the most significant. It has been reported before that IR imaging can under-report temperatures, and also under-report the *change in temperature with position* [1, 2]. This will result in a reported thermal conductivity that is too high, exactly as seen for Si. It should be noted that the opposite trend was seen for the SiC wafer, although to a smaller percentage degree. It may be that there is a combination of this and an additional systematic issue. To address this last issue, we plan to measure a wafer coated with an IR opaque and emissive substance. This is known to reduce error in temperature measurement and may bring the data in line with expectations.

CONCLUSIONS

In conclusion, we have shown that an IR microscope can be used to estimate the lateral thermal conductivity of a substrate, using existing material without additional processing. Sources of error are investigated and data are compared to expectations. We find that the technique as reported can generate useful data, but that there are sources of error not addressed by the concerns we were able to test. We plan to test coating the wafer to change the IR response next to attempt to improve this technique.

ACKNOWLEDGEMENTS

The authors would like to thank Joe Breedlove and Paul Cassity for assisting with metal deposition and material etching. This collaborative effort with RFMD was supported by contract # FA8650-05-C-5411.

REFERENCES

[1] Accurate Channel Temperature Measurement in AlGaN/GaN HEMT Devices and its Impact on Accelerated Lifetime Predictive Models", B. Claflin et al., CS MANTECH in Tampa, FL, May 18-21, 2009.

[2] A. Sarua, H. Ji, M. Kuball, M. J. Uren, T. Martin, K. P. Hilton, and R. S. Balmer, IEEE Trans. Electron Devices vol. 53, pp. 2438-2447, 2006.

[3] *ANSYS/Mechanical Software Suite*, ANSYS, Inc., Canonsburg, PA.

[4] D.A. Benson, D. Bowman, W. Filter, R. Mitchell, "Design and Characterization of Microscale Heater Structures for Test Die and Sensor Applications", IEEE InterSociety Conference on Thermal Phenomena, pp. 434-441, 1998.

[5] www.quantumfocus.com.

[6] Young, Hugh D., University Physics, 7th Ed., Addison Wesley, 1992.

ACRONYMS

HEMT: High Electron Mobility Transistor
GSG: Ground-Signal-Ground
IR: Infra-red
CuBe: Copper Beryllium
WBG: Wide Bandgap